Measurement of the neutrino asymmetry in the β decay of laser-cooled, polarized ^{37}K

D. Melconian [a,b,*], J.A. Behr [c], D. Ashery [d], O. Aviv [d], P.G. Bricault [c], M. Dombsky [c], S. Fostner [c], A. Gorelov [a], S. Gu [c], V. Hanemaayer [c], K.P. Jackson [c], M.R. Pearson [c], I. Vollrath [c]

[a] *Department of Physics, Simon Fraser University, Burnaby, British Columbia, Canada V5A 1S6*
[b] *Department of Physics, University of Washington, Seattle, WA 98195, USA*
[c] *TRIUMF, 4004 Wesbrook Mall, Vancouver, British Columbia, Canada V6T 2A3*
[d] *Tel Aviv University, 69978 Tel Aviv, Israel*

Abstract

A measurement of the neutrino asymmetry is presented which represents the first search for new physics using polarized radioactive atoms initially cooled and confined in a magneto-optical trap. Optical pumping and photoionization techniques are used to generate and measure, in situ, a highly spin-polarized (96.5(0.8)%) sample of the short-lived β^+-emitter ^{37}K. The angular distribution of neutrinos from this polarized decay, inferred from the daughter recoil asymmetry, is used to search for a hypothetical $V + A$ current in the weak interaction. We find the ν asymmetry parameter to be $B_\nu = -0.755 \pm 0.020(\text{stat}) \pm 0.013(\text{syst})$, in agreement with the standard model's purely $V-A$ interaction.
© 2007 Elsevier B.V. All rights reserved.

1. Introduction

Many extensions to the standard model (SM) propose that parity symmetry, which is maximally violated by the weak interaction, is restored at some higher energy scale [1–3]. In the simplest manifest left–right symmetric models [4], the SM electroweak gauge group $SU(2)_L \otimes U(1)$ is extended to include a right-handed sector and is given identical couplings, CKM matrices and neutrino sectors. Only three new parameters are introduced: the mass of the new W_R boson that couples to right-handed neutrinos, a *CP*-violating phase, ω, and an angle, ζ, describing the level of mixing between the weak ($W_{L,R}$) and mass eigenstates ($W_{1,2}$, with masses $M_{1,2}$):

$$W_L = W_1 \cos\zeta - W_2 \sin\zeta,$$
$$W_R = (W_1 \sin\zeta + W_2 \cos\zeta)e^{i\omega}. \tag{1}$$

Nuclear β decay is sensitive to the W_R either directly or through mixing with the W_L, with dependencies that scale like M_1^2/M_2^2 and $\tan\zeta$, respectively. In more general models, the two sectors have different couplings, CKM matrices and neutrinos (though the $\nu^{(R)}$ must be light enough to be produced), which increases the parameter space [5]. This makes limits from β decay, μ decay and collider searches complementary because their dependencies differ [6].

A number of active research programs [7–10] continue searching for such right-handed currents. The advent of neutral atom trapping techniques [11] in the mid-1980s introduced a powerful new technique for precision β decay studies because they provide a backing-free, cold, localized source of isotopically-selected atoms. Recently, two experiments using a magneto-optical trap (MOT) have produced measurements of the $\beta - \nu$ correlation parameter [12,13]. As a first step toward searching for right-handed currents, the β asymmetry of ^{82}Rb has been observed using a magnetic time-orbiting potential trap [14].

* Corresponding author.
E-mail address: melcon@npl.washington.edu (D. Melconian).

2. Principle of the measurement

In this Letter we present a novel technique combining optical pumping (OP) with a MOT to produce a highly spin-polarized sample of laser-cooled atoms. These near-ideal conditions are utilized to make a precision measurement of the neutrino asymmetry parameter, B_ν, in the β decay of a polarized nucleus. This parameter is an observable in the angular distribution of the decay [15]:

$$
\frac{d^5\Gamma_{\text{angular}}}{dE_e\,d\Omega_e\,d\Omega_\nu} \propto \left\{ 1 + a_{\beta\nu}\frac{\vec{p}_e \cdot \vec{p}_\nu}{E_e E_\nu} + b\frac{m_e}{E_e} \right.
$$
$$
+ P\hat{i} \cdot \left[A_\beta \frac{\vec{p}_e}{E_e} + B_\nu \frac{\vec{p}_\nu}{E_\nu} + D\frac{\vec{p}_e \times \vec{p}_\nu}{E_e E_\nu} \right]
$$
$$
+ c\left[\frac{\vec{p}_e \cdot \vec{p}_\nu}{3E_e E_\nu} - \frac{(\vec{p}_e \cdot \hat{i})(\vec{p}_\nu \cdot \hat{i})}{E_e E_\nu} \right]
$$
$$
\left. \times \left[\frac{I(I+1) - 3\langle(\vec{I}\cdot\hat{i})^2\rangle}{I(2I-1)} \right] \right\}, \tag{2}
$$

where $(E_l, \vec{p}_l)$ are the four-momenta of the leptons, and $P = |\vec{I}|/I$ is the nuclear polarization of the parent nucleus along a direction $\hat{i}$. The values for the correlation parameters $a_{\beta\nu}, b, c, A_\beta, B_\nu$ and D depend explicitly on fundamental symmetries of the weak interaction [15]. They are also potentially sensitive to new physics; in particular, a non-zero value for D would violate time-reversal symmetry, while the β and ν asymmetry parameters, A_β and B_ν, can be used to search for right-handed currents. B_ν defines the dependence of the polarized angular distribution on the correlation between $\vec{p}_\nu$ and the initial nuclear polarization. In the present experiment this dependence is measured by detecting the nuclear recoils in coincidence with βs observed perpendicular to $\hat{i}$. Given this particular geometry and since the decay is of a free atom laser-cooled so as to be initially at rest, the relevant component of $\vec{p}_\nu$ is of equal magnitude and opposite sign to that of the recoil $\vec{p}_{\text{recoil}}$. Finite detector acceptances and averaging over E_β complicate the analysis, but the observed $\hat{x}$ recoil asymmetry (defined below) remains closely related to $\cos\theta_{\hat{i},\nu}$, and so is primarily sensitive to B_ν.

The ν asymmetry has previously been measured only in ^{19}Ne [16] (to 14%) and the neutron [17] (to 0.4%). The focus of this work is the mixed Fermi/Gamow–Teller β^+ decay of the mirror nucleus ^{37}K [18] which has a 97.89(11)% $I^\pi = \frac{3}{2}^+ \to \frac{3}{2}^+$ branch to the ground state with $Q_{EC} = 6.1475(2)$ MeV. For this transition and within the SM, $A_\beta^{\text{SM}} = -\frac{2}{5}\lambda(\sqrt{15} - \lambda)/(1 + \lambda^2)$ and $B_\nu^{\text{SM}} = -\frac{2}{5}\lambda(\sqrt{15} + \lambda)/(1 + \lambda^2)$ where λ is the ratio of Gamow–Teller to Fermi matrix elements, $\lambda = g_A M_{\text{GT}}/g_V M_F$. The magnitude $|\lambda| = 0.5754(16)$ was inferred from the measured ft value [19]. The only other transition of appreciable strength is a pure GT branch to the $\frac{5}{2}^+$ 2.8 MeV level in ^{37}Ar at 2.07(11)%, with all others $< 0.25\%$ [20].

We define the experimental ^{37}Ar-recoil position asymmetry along $\hat{x}$ to be

$$
\mathcal{A}_{\text{Ar}}(x) \equiv \frac{N^+_{\text{Ar}}(x) - N^-_{\text{Ar}}(x)}{N^+_{\text{Ar}}(x) + N^-_{\text{Ar}}(x)}, \tag{3}
$$

where $N^\pm_{\text{Ar}}$ is the observed number of recoils for polarization along $\hat{i} = \pm\hat{x}$. This asymmetry, which scales like PB_ν, is compared to a Monte Carlo (MC) simulation which calculates the expected asymmetry after integrating over β energies and the detector acceptances. The other non-zero correlations, $a_{\beta\nu}$ and c, do not give rise to an asymmetry but do contribute to the denominator of Eq. (3) and are therefore included in the simulations. Recoil-order corrections (given by CVC) [21] and estimates of radiative [22] corrections to the observables are $\lesssim 0.25\%$, which is negligible compared to the present experimental uncertainty and so are not included in the present analysis.

3. The experiment

The radioactive beam facility at TRIUMF, ISAC, provided 6×10^7 ^{37}K$^+$ ions/s to the TRIUMF Neutral Atom Trap facility [23]. Many of the same techniques used by our group to measure the $\beta - \nu$ correlation parameter in ^{38m}K continue to be utilized in the present experiment (see [12] and references therein). The mass-separated 30 keV ion beam was implanted into a heated Zr foil which neutralized and released [24] the short-lived ($t_{1/2} = 0.972$ s) ^{37}K atoms into a vapour-cell 'collection' MOT. We use a 30 ms pulse of laser light every 700 ms to gently push these cooled, isotopically selected atoms with 75% efficiency directly into a 2nd 'detection' MOT [25] where we house our particle detectors (see Fig. 1). We wait 50 ms for the atoms to collect before initiating the polarization and counting sequence.

3.1. Particle detection

βs emitted perpendicular to the polarization axis are observed by a double-sided Si-strip detector (DSSSD) plus BC408 plastic scintillator β-telescope as shown in Fig. 1(a). The DSSSD provides a ΔE signal with 0.1×0.1 mm^2 position information, while the 6.5 cm thick scintillator stops the β and measures the full energy. The recoils are detected in a microchannel plate (MCP) detector consisting of three 600 μm thick plates in the Z-stack configuration, biased at ≈ 1 kV/plate. The resistive-anode readout was calibrated with an α source and mask to within ± 0.1 mm at the edges of the active area (defined by a 2.4 cm diameter passive collimator) where non-linearities are largest; the position resolution of the device was found to be ± 0.25 mm. Charged recoils are accelerated and separated into different charge states by time-of-flight with respect to the β trigger using a uniform electric field of $\vec{E} = -810(10)\hat{z}$ V/cm. Both of these detectors have already been very well characterized from the analysis of our unpolarized ^{38m}K data [12].

In extending the techniques used in our scalar search [12] to this spin-polarized case, two BC408 + CaF$_2$(Eu) "phoswich" detectors were added to the system as shown in Fig. 1(b) to observe βs emitted along the polarization axis. Both the plastic (1″ in diameter and 2 mm thick) and CaF$_2$(Eu) (1.2″ in diameter and 20 mm thick) are read out by the same photomultiplier tube, with the signals separated by short and long gates (32 ns and 5 μs, respectively). The βs have been shown to be clearly
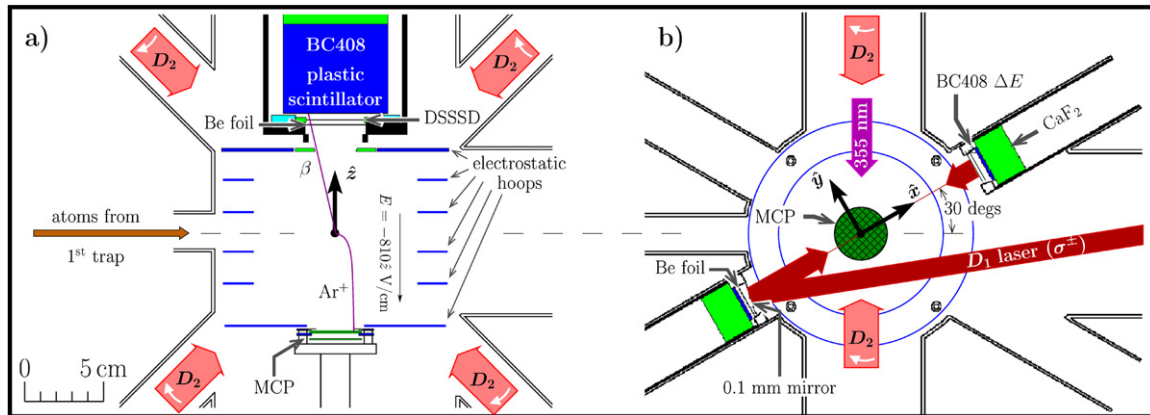
Fig. 1. (Colour online.) Top (a) and side (b) views of the 2nd chamber housing the 'detection' MOT, electrostatic hoops and particle detectors (see text). The top view shows the recoil MCP detector and the DSSSD + scintillator telescope used to measure B_ν; the phoswich detectors are out of the plane in (a), but are seen in the side view (b) which shows the geometry as viewed from the trap along $-\hat{z}$ towards the MCP. All three β detectors have thin Be foils to separate them from the 3×10^{-10} Torr vacuum of the trapping chamber. The trapped atoms are localized within a 3 mm FWHM cloud at the centre of the apparatus. Also shown are the trapping (D_2), optical pumping (D_1) and photoionization (355 nm) laser beams (see also Fig. 2). The polarization axis, defined by the laser exciting the D_1 transition, is along $\pm \hat{x}$.
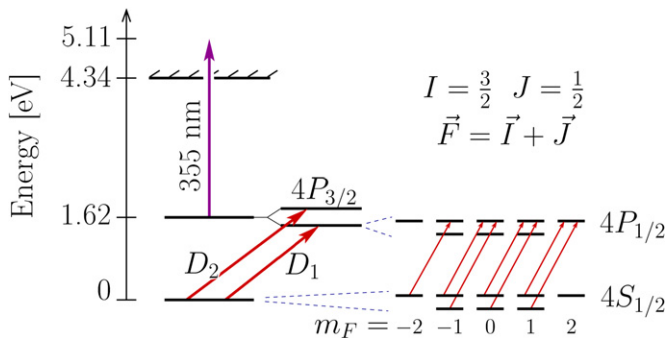

Fig. 2. (Colour online.) Fine and hyperfine structure of ^{37}K showing the relevant laser transitions. Circularly polarized light brought in along $\pm \hat{x}$ (see Fig. 1) and tuned to the D_1 transition pump atoms into the $F = 2$, $m_F = \pm 2$ hyperfine state, resulting in a very high average cloud polarization. The 355 nm laser continually probes the excited state population by photoionizing atoms from the excited P states.

resolved from backgrounds in a plot of the phoswich E vs. ΔE spectrum, and so these detectors provide a clean tag for β events, even though distortions and the noise level is higher in these detectors compared to the DSSSD + scintillator telescope.

3.2. Atomic techniques

The lasers and energy levels involved in the trapping and optical pumping are depicted in Fig. 2. We trap using three pairs of counter-propagating laser beams tuned -26 MHz to the red of the D_2 transition (766.7 nm) with circular polarizations as shown in Fig. 1. Fig. 2 shows the principle of optical pumping [26] using the D_1 transition (769.9 nm), in this case using σ^+ polarized light: with repeated absorptions and subsequent spontaneous decays, atoms accumulate in the $4S_{1/2}|F\ m_F = \pm 2\rangle$ fully-stretched state. Since the nuclear (I) and atomic spins (J) are coupled by the hyperfine interaction, this state corresponds to complete atomic *and* nuclear polarization.

To compensate the small ellipticity produced in the D_1 light from reflection off the $11.5°$ mirror, we oriented an identically coated dielectric mirror outside the vacuum chamber $11.5°$ in the opposite plane. The result is a highly-circularly polarized laser beam with a Stokes parameter $S_3 \geqslant 0.9985$.

The two laser frequencies needed to optically pump both $S_{1/2}$ ground states are generated by rf sidebands on the laser diode [27] 1 MHz greater than the 240.3 MHz ground state hyperfine splitting. We have shown off-line using stable ^{41}K that this detuning completely destroys dark-state coherences, which could otherwise produce poorly polarized atoms with vanishing fluorescence [28].

We monitor critical aspects of the average polarization and location of the cloud by photoionizing about one out of every thousand atoms. We use a 355 nm laser with 0.6 ns time pulses, 20 µJ/pulse at a repetition rate of 10 kHz. A photoionized ^{37}K$^+$ ion gets swept by the electric field onto the MCP and is observed in coincidence with the laser pulse, so it is completely distinguished from events produced by β decay. The 355 nm light only has enough energy to photoionize atoms from the excited states (see Fig. 2), so the photoionization rate is proportional to the atomic excited state population. Rayleigh scattering, which can destroy polarization and heat the atoms, has a cross-section of about a barn, whereas non-resonant photoionization is known to have a cross-section of 7MB [29]. Thus a 355 nm photon either ionizes an atom and removes it from the system, or it does nothing to one part in a million. Uniform illumination of the cloud was ensured by making the beam diameter 25 mm, much larger than the cloud dimensions. In this way, we non-destructively image the cloud in all three dimensions ($\hat{x}$, $\hat{y}$-MCP positions, and the time-of-flight with respect to the laser pulse provides the $\hat{z}$ component). The excited-state population provides the polarization monitor, as discussed in Section 4.1.

The D_2 trapping beams have both positive and negative circular polarizations which destroys any polarization of the atomic cloud, so we use an alternating trap/optical pumping

cycle to polarize the laser-cooled atoms. To begin each cycle, atoms are trapped in the detection MOT for 2.1 ms. The trapping quadrupole B-field is then ramped down and, when completely off, the trapping D_2 laser beams are extinguished at which point the atoms ballistically expand (with $T_{trap} \approx 6$ mK) from an initial cloud size of $\lesssim 3$ mm FWHM. After a 10 μs delay, the D_1 laser illuminates the cloud to optically pump and polarize the atoms. A residual $B_{op} = -2$ G field from the trim coils of the trapping field aligned with the optical pumping axis is always left on to suppress the depolarizing effects of (transverse) ambient fields. In order to re-trap atoms before they expand too far, we turn off the D_1 beam and turn the MOT back on after 1.15 ms of optical pumping, starting the trap/OP cycle again. We alternate positive and negative polarizations every 4.5 seconds by switching the $\sigma^\pm$ polarization of the D_1 laser.

4. Results and data analysis

4.1. Nuclear polarization

Fig. 3 shows the photoion event rate during the optical pumping part of the cycle. At the start, we see large number of photoions as the atoms make a biased random walk from equal sublevel populations to an accumulation into the $4S_{1/2}|F\ m_F = \pm 2\rangle$ stretched state. The number of photoions quickly diminishes as the cloud becomes fully polarized because there is no $|m_{F'}| = 3$ sublevel in the $4P_{1/2}$ manifold to excite from the stretched ground state. After $\gtrsim 200$ μs, a steady-state is achieved and it is the final photoion rate compared to the initial spike which provides us with a sensitive probe of the polarization: any residual photoions must arise from atoms not in the $|m_F| = 2$ fully-polarized state. Using a rate equation model, the excited state populations are fit to the photoion data, corresponding to a slightly model-dependent fit of the average nuclear polarization of the *same atoms that are decaying*. We found $\langle P_{\sigma+}\rangle = (+97.7 \pm 0.4^{+0.2}_{-0.5})\%$ and $\langle P_{\sigma-}\rangle =$
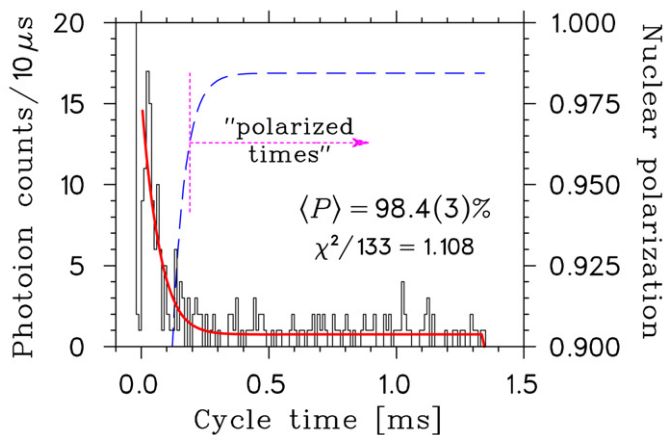

Fig. 3. (Colour online.) Typical photoion spectrum (histogram) during the optical pumping part of the trap/polarization cycle, and fit to a rate equation model (solid line). The rate equations describe the time-evolution of the magnetic sublevel populations, providing us with a measurement of the cloud's average polarization. The dashed line shows the value of the polarization calculated by the rate-equation model.
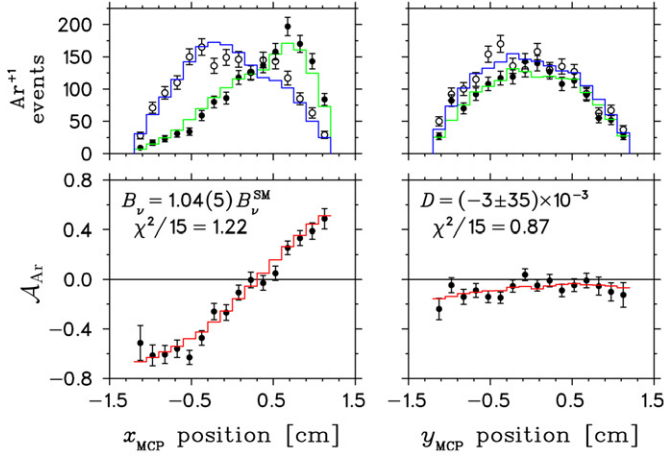
$(-95.8 \pm 1.0^{-0.4}_{+1.3})\%$ during "polarized times" when we make our asymmetry measurements. The second uncertainty is systematic, dominated by the normalization of the photoion rate at the start of the OP process. We have subsequently shown that depolarizing effects and the difference between $\sigma^\pm$ polarizations are greatly reduced when a better B_{op}-field is made using a Helmholtz coil for optical pumping. This is consistent with the high quality of the circular polarization of the optical pumping light, and shows that stray magnetic fields are the dominant source of depolarizing effects in this experiment.

4.2. Spin-polarized observables

The phoswich detectors were meant to observe the β singles so as to make an A_β measurement based on the change in count rates between the two polarization states; unfortunately we found, from comparison with the known radioactive decay lifetime, that a significant number of atoms were ejected from the trapping region (up to 25%). This presented a large background which could be modelled and accounted for, but not well enough to make a precision measurement of A_β. The electric field suppresses ions originating from the walls, so a decay event originating outside of the trapping region cannot trigger both the recoil and one of the β detectors. This was confirmed by intentionally ejecting atoms to the walls. Therefore, β-Ar coincidences do not suffer from the backgrounds of the β singles and can be used to perform a very clean measurement of spin-polarized observables.

The spatial dependence of the ions on the MCP in coincidence with a β in one of the phoswich detectors is sensitive to new physics through a combination of A_β and B_ν that is only weakly dependent on λ (and therefore insensitive to isospin mixing and the value of V_{ud}). This observable vanishes by helicity arguments when the β is emitted opposite to the nuclear spin and the ν parallel. However, due to the kinematics of the decay and the detector acceptances (particularly the recoil detector), there are presently insufficient statistics for a precision measurement of this observable.

The DSSSD + scintillator–MCP coincidences are also very clean, and are primarily sensitive to the value of B_ν as discussed in Section 2. We recorded 1.8×10^4 polarized events of this type in two blocks of runs totalling 35 hours of on-line data collection. Both sets of runs were separately characterized using the photoion data giving us the polarization and cloud parameters needed as inputs for the MC simulations. The MC generates events according to Eq. (2) using the SM values of all the parameters, and includes the weaker pure GT branches to excited states. Tracking of the βs and γs was done using GEANT [30] to account for scattering and to simulate the response functions of the detectors. A software threshold of 500 keV was imposed on the energy deposited in the plastic scintillator (both in the data and the MC) due to concerns regarding the effectiveness of GEANT to simulate low-energy βs as well as to avoid backgrounds from the Compton edge of 511-keV annihilation photons. The position dependence of $\mathcal{A}_{Ar}$ is defined by the β-telescope and MCP acceptances and by the electric field, while the magnitude is proportional to

Fig. 4. (Colour online.) MCP projections (closed/open circles are positive/negative polarization) and asymmetries (points) for DSSSD + scintillator–Ar^{+1} coincidences during "polarized times". The $\hat{x}$-asymmetries (left) are sensitive to B_ν while the $\hat{y}$-asymmetries (right) are sensitive to D. The results of fitting to the MC simulations are overlaid as histograms in all cases. The $\sigma^{\pm}$ distributions in $\hat{x}$ are not mirror-images of each other because the trap was not perfectly aligned with the centre of the MCP and because of the suppressed efficiency centred at $x_{MCP} \approx +3$ mm (see text).

$\kappa \equiv \frac{1}{2}(\langle P_{\sigma+}\rangle - \langle P_{\sigma-}\rangle)B_\nu/B_\nu^{SM} \sim 1$. The polarized data and comparison to simulations are shown in the top-left/right panel of Fig. 4 where we plot a typical example of the $\sigma^{\pm}$ MCP $\hat{x}/\hat{y}$-position spectra of DSSSD + scintillator–Ar^{+1} coincidences. The corresponding asymmetries are shown below. The magnitude of the observed $\hat{x}$-asymmetry, κ, was fit to each of the three charge states for both data sets. With P determined independently, these fits to κ correspond to a measurement of B_ν. A fit to the sum of charge states $+1$, $+2$ and $+3$ yielded results consistent with the average of each fit independently. Uncertainties from fits to the $\hat{y}$-asymmetry are too large to provide a useful D measurement in light of the 10^{-3} limits from neutron [31] and ^{19}Ne [32] decays. The slight offset, well-reproduced by the MC, is a result of unequal statistics in the two polarization states. The fact that no $\hat{y}$-asymmetry is seen provides us with a useful cross-check of systematics in the B_ν measurement, particularly the alignment of the optical pumping laser with the $\hat{x}$-axis of the MCP.

The list of uncertainties for the B_ν measurement are given in Tables 1 and 2. Table 1 lists the uncertainties that were separately determined for the two data sets while Table 2 lists those that were the same throughout the experiment and therefore were common to both. The total uncertainty is presently dominated by the statistical uncertainty of the fit to κ. The cloud position and velocity are correlated systematics as are the cloud temperature and size; the latter is not as large a systematic because it perturbs the 2nd moment of the spatial distribution whereas shifts in the position or velocity of the cloud can easily generate a false asymmetry. Typically, position and velocity shifts were consistent with zero to within uncertainties of ± 0.5 mm and ± 7 cm/s, respectively. The binning error is from non-Gaussian statistics and would decrease with more counts.

The dominant common systematic uncertainty is the position calibration of the recoil detector. A passive collimator defined

Table 1
Uncertainties in the B_ν measurement that are separate for the two data sets

Source	$\sigma_\kappa^{stat}/\kappa$ [%]		Source	$\sigma_\kappa^{syst}/\kappa$ [%]	
	1st	2nd		1st	2nd
Asym. fit	± 4.0	± 3.1	Cloud pos/vel	$^{+1.5}_{-1.0}$	$^{+1.0}_{-1.3}$
Polarization	∓ 0.7	∓ 0.8	Cloud size/temp	$^{+0.5}_{-0.0}$	$^{+0.3}_{-0.5}$
			Binning	$^{+0.4}_{-0.5}$	$^{+0.2}_{-0.3}$
Total stat	± 4.1	± 3.2	Total syst	$^{+1.8}_{-1.1}$	$^{+1.0}_{-1.6}$

Table 2
Systematic uncertainties in the B_ν measurement that are common to the two data sets

Source	$\sigma_{B_\nu}/|B_\nu|$ [%]
MCP position calibration	$^{+0.7}_{-1.3}$
MCP efficiency	$^{+0.4}_{-0.5}$
Polarization	$^{+0.2}_{-0.7}$
$\hat{x}_{MCP}$–OP alignment	$^{+0.4}_{-0.1}$
Electric field	± 0.2
E_β threshold	± 0.1
Total	$^{+1.0}_{-1.9}$

the active area of the MCP, but since we are taking an asymmetry as a function of position, we are very sensitive to this calibration. Variations in the efficiency of the MCP over its active area is a source of uncertainty only because our front plate was damaged by excessive ^{41}K photoion collection during off-line development. The relative efficiency was reduced by as much as 50% in a region ≈ 4 mm FWHM centred at $x_{MCP} = 3$ mm; ordinarily this would not contribute because the recoiling ions are accelerated from $\leqslant 430$ eV to ≈ 5 keV where the efficiency is known to be homogeneous and constant to 0.6% [12].

5. Conclusions

Combining the results from the three charge states (either independently or summed together) of the two data sets, we find $B_\nu = -0.755 \pm 0.020(\text{stat}) \pm 0.013(\text{syst})$. This result agrees with the SM prediction of $B_\nu^{SM} = -0.7692(15)$ assuming $\lambda = +0.5754(16)$; if λ was negative B_ν^{SM} would be $+0.5702$, so our results unambiguously determine the sign of λ to be positive.

Future prospects are promising because we have identified and are able to reduce all of our largest uncertainties. We have achieved $(99.6 \pm 0.2)\%$ polarization in ^{41}K [28], and expect similar results in ^{37}K. Furthermore, with some off-line development, we will be able to reduce the cloud temperature and movements associated with switching between trapping and polarizing. This would also likely reduce the number of atoms ejected from the trapping region and would make an A_β measurement using the β singles more viable. A larger MCP would increase our collection efficiency, which would be especially useful for phoswich–MCP coincidences. By placing a largely
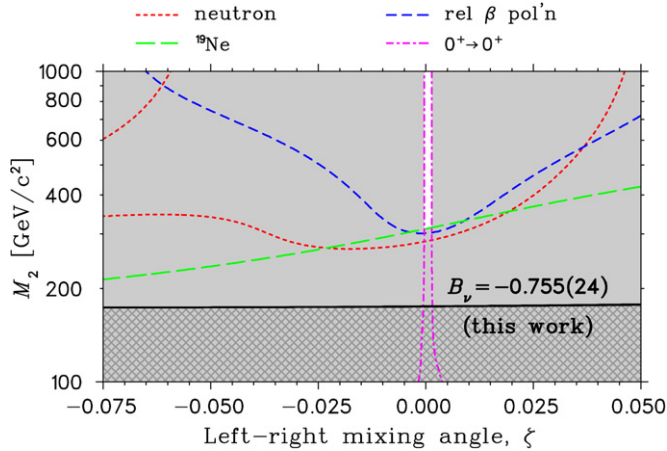
Fig. 5. (Colour online.) The 90% C.L. limits on right-handed current parameters from semi-leptonic decays in the manifest left–right symmetric model (excluded regions shaded). All limits shown are consistent with the SM prediction of $\zeta = 0$ and $M_2 \to \infty$.

open-area ($\approx$90%), permanent mask on the front plate of the recoil detector, we will have an in situ calibration of the MCP position. This will minimize uncertainties from the position calibration as well as the alignment of the OP beam with the $\hat{x}$-axis of the MCP.

Within the framework of the manifest left–right symmetric model, this 3% measurement of B_ν corresponds to the 90% C.L. limits on the mass and mixing angle shown in Fig. 5. The value of V_{ud} from $0^+ \to 0^+$ decays [33] and assuming unitarity of the CKM matrix [17] puts the most stringent limits on the mixing angle. Other limits from nuclear β decay include: the β asymmetry of ^{19}Ne [34]; the relative β polarization asymmetries summarized in [7]; and the decay of the neutron [17]. Limits from μ^+ decay, high-energy colliders and astronomical constraints are discussed in the recent review of Ref. [6]. Fig. 5 shows that the current B_ν result (excludes hatched region) does not yet provide a competitive test of the standard model: our limit of $M_2 > 180 \, \text{GeV}/c^2$ is already excluded by other experiments. However, with the improvements to our system discussed above, we could achieve a 0.5% measurement of B_ν which would reach limits on M_2 comparable to the world average from semi-leptonic decays. In addition, with higher statistics and a larger recoil detector, we will be able to make use of the phoswich–MCP coincidences as an independent probe of right-handed currents. Limits derived from a combined measurement of this and B_ν would be complementary to present limits.

References

[1] J.C. Pati, A. Salam, Phys. Rev. D 10 (1974) 275.
[2] G. Senjanovic, R.N. Mohapatra, Phys. Rev. D 12 (1975) 1502.
[3] P. Herczeg, Prog. Part. Nucl. Phys. 46 (2001) 413.
[4] M.A.B. Bég, et al., Phys. Rev. Lett. 38 (1977) 1252.
[5] P. Langacker, S.U. Sankar, Phys. Rev. D 40 (1989) 1569.
[6] N. Severijns, M. Beck, O. Naviliat-Cuncic, Rev. Mod. Phys. 78 (2006) 991.
[7] E. Thomas, et al., Nucl. Phys. A 694 (2001) 559.
[8] H. Abele, Nucl. Instrum. Methods Phys. Res. A 440 (2000) 499.
[9] J.C. Hardy, I.S. Towner, Phys. Rev. C 71 (2005) 055501.
[10] A. Gaponenko, et al., Phys. Rev. D 71 (2005) 071101(R).
[11] E.L. Raab, et al., Phys. Rev. Lett. 59 (1987) 2631.
[12] A. Gorelov, et al., Phys. Rev. Lett. 94 (2005) 142501.
[13] N.D. Scielzo, et al., Phys. Rev. Lett. 93 (2004) 102501.
[14] S.G. Crane, et al., Phys. Rev. Lett. 86 (2001) 2967.
[15] J.D. Jackson, S.B. Treiman, H.W. Wyld, Nucl. Phys. 4 (1957) 206.
[16] F.P. Calaprice, et al., Phys. Rev. 184 (1969) 1117, $B_\nu = -0.90(13)$ for ^{19}Ne.
[17] W.-M. Yao, et al., J. Phys. G 33 (2006) 1. The PDG's recommended values are: $\tau = 885.7(8)$ s, $A_\beta = -0.1173(13)$ and $B_\nu = 0.9824(40)$ [neutron] $V_{us} = 0.2257(21)$ and $V_{ub} = 0.0036(7)$ [CKM unitarity].
[18] P.M. Endt, Nucl. Phys. A 633 (1998) 1.
[19] G.C. Ball, Proceedings of the 15th Lake Louise Winter Institute, World Scientific, Singapore, 2000.
[20] E. Hagberg, et al., Phys. Rev. C 56 (1997) 135.
[21] B.R. Holstein, Rev. Mod. Phys. 46 (1974) 789.
[22] F. Glück, Phys. Lett. B 436 (1998) 25. We use the calculation for B_ν in the neutron as an order of magnitude estimate for ^{37}K.
[23] M. Dombsky, P. Bricault, V. Hanemaayer, Nucl. Phys. A 746 (2004) 32c.
[24] D. Melconian, et al., Nucl. Instrum. Methods Phys. Res. A 538 (2005) 93.
[25] T.B. Swanson, et al., J. Opt. Soc. Am. B 15 (1998) 2641.
[26] P. Tremblay, C. Jacques, Phys. Rev. A 41 (1990) 4989.
[27] C.J. Myatt, N.R. Newbury, C.E. Wieman, Opt. Lett. 18 (1993) 649.
[28] S. Gu, et al., Opt. Commun. 220 (2003) 365.
[29] I.D. Petrov, V.L. Sukhorukov, E. Leber, H. Hotop, Eur. Phys. J. D 10 (2000) 53.
[30] GEANT Detector Description and Simulation Tool, version 3.2114, Cern (1994).
[31] L.J. Lising, et al., Phys. Rev. C 62 (2000) 055501.
[32] A.L. Hallin, et al., Phys. Rev. Lett. 52 (1984) 337.
[33] W.J. Marciano, A. Sirlin, Phys. Rev. Lett. 96 (2006) 032002.
[34] F.P. Calaprice, et al., Phys. Rev. Lett. 35 (1975) 1566.